Inorg. Chem. **2004**, *43*, 5120–5127

Selective Dehydrogenation of Amines with Respect to Coordination Geometry: Different Oxidation Products of Tricyano[bis(2-pyridylmethyl)amine]ferrate(II) between *mer*- and *fac*-Isomers

Masafumi Goto, Nobuhiro Koga, Yasuhiko Ohse, Yuka Kudoh, Michiko Kukihara, Yoshinori Okuno, and Hiromasa Kurosaki*

Graduate School of Pharmaceutical Sciences, Kumamoto University, Oe-honmachi 5-1, Kumamoto, 862-0973, Japan

Received November 7, 2003

Both the *fac*- and *mer*-isomers of tricyano[bis(2-pyridylmethyl)amine = 2-DPA]ferrate(II) were isolated and their spectroscopic properties compared. The *fac*-isomer was converted to the corresponding iron(III) complex under acidic conditions. Oxidation of the ferrate(II) complexes with ammonium peroxodisulfate yielded the *mer*-isomer of the dehydrogenated ferrate(II) compound, but only the metal-oxidized iron(III) complex for the *fac*-isomer was produced under neutral or basic conditions. Electrochemical measurements confirmed this difference in the oxidation behavior, in which the nature of the coordination governs the ease of oxidative dehydrogenation.

Introduction

The metal-assisted oxidation of peptides, one of the causes of damage to proteins, represents a putative cause of aging.[1] It has been proposed that the reaction of a lysine side chain with proline, assisted by iron, is involved in this aging.[1] Reactions involving the metal-assisted oxidative dehydrogenation of amines have been extensively studied using group-8 triads, Fe,[2−8] Ru,[9−14] and Os,[15,16] which have been reviewed by Keene.[17]

The general mechanism involves the oxidation of metal ions to a high-valent state, followed by their base-promoted disproportionation.[4,11,13,18] The amines employed ranged from simple amines to diamines and macrocyclic tetraamines. Secondary amines appear to be about 3000 times more susceptible to disproportionation than primary amines.[4]

Oxidative dehydrogenation or disproportionation would be expected to be dependent on the coordination mode of the ligand. On the basis of this assumption, we initiated a study designed to shed light on the relationship between disproportionation and the coordination mode, i.e. the influence of geometrical isomerism on oxidative dehydrogenation. Tridentate or tetradentate amines coordinated to low-spin iron(II) should exist in the form of geometric isomers. This requires the preparation and separation of the possible geometrical isomers of tridentate or tetradentate (amine)-metal complexes. The tricyano[bis(2-pyridylmethyl)amine = 2-DPA]ferrate(II) has been reported to yield a mixture of

* Author to whom correspondence should be addressed. E-mail: ayasaya@gpo.kumamoto-u.ac.jp. Tel: +81 (Japan)-96-371-4315. Fax: +81 (Japan)-96-371-4314.

(1) Stadtman E. R. *Science* **1992**, *257*, 1220−1224.
(2) Pohl, K.; Wieghardt, K.; Kaim, W.; Steenken S. *Inorg. Chem.* **1988**, *27*, 440−447.
(3) Kuroda Y.; Tanaka, N.; Goto, M.; Sakai, T. *Inorg. Chem.* **1989**, *28*, 2163−2169.
(4) Goto, M.; Takeshita, M.; Kanda, N.; Sakai, T.; Goedken, V. L. *Inorg. Chem.* **1985**, *24*, 582−587.
(5) Goto, M.; Takeshita, M.; Sakai, T. *Bull. Chem. Soc. Jpn.* **1981**, *54*, 2491−2495.
(6) Goedken, V. L. *J. Chem. Soc. Chem. Commun.* **1972**, 207−208.
(7) Goedken, V. L.; Busch, D. H. *J. Am. Chem. Soc.* **1972**, *94*, 7355−7363.
(8) Maria da Costa Ferreria, A. M.; Toma, H. E. *J. Chem. Soc., Dalton Trans.* **1983**, 2051−2055.
(9) Yamaguchi, M.; Machiguchi, K.; Mori, T.; Kikuchi, K.; Ikemoto, I.; Yamagishi, T. *Inorg. Chem.* **1996**, *35*, 143−148.
(10) Yamaguchi, M.; Yamagishi, T. *Inorg. Chem.* **1993**, *32*, 2981−2982.
(11) Keene, F. R.; Ridd, M. J.; Snow, M. R. *J. Am. Chem. Soc.* **1983**, *105*, 7075−7081.
(12) Bernhard, P.; Sargeson, A. M. *J. Am. Chem. Soc.* **1989**, *111*, 597−606.
(13) Bernhard, P.; Bull, D. H.; Bürgi, H.-B.; Osvath, P.; Raselli, A.; Sargeson, A. M. *Inorg. Chem.* **1997**, *36*, 2804−2815.
(14) Cabort, A.; Therrien, B.; Stoeckli-Evans, H.; Bernauer, K.; Süss-Fink, G. *Inorg. Chem. Commun.* **2002**, *5*, 787−790.
(15) Patel, A.; Ludi, A.; Bürgi, H−B.; Raselli, A.; Bigler, P. *Inorg. Chem.* **1992**, *31*, 3405−3410.
(16) Lay, P. A.; Sargeson, A. M.; Skelton, B. W.; White, A. H. *J. Am. Chem. Soc.* **1982**, *104*, 6161−6164.
(17) Keene, F. R. *Coord. Chem. Rev.* **1999**, *187*, 121−149.
(18) Constable, E. C. *Metals and Ligand Reactivity-An Introduction to the Organic Chemistry of Metal Complexes*; VCH Verlag: Weinheim, Germany, 1996; Chapter 9.3.

10.1021/ic035289a CCC: $27.50 © 2004 American Chemical Society
Published on Web 07/03/2004

mer- and *fac*-isomers, which are isolable.[19] This report describes their preparation and a comparison of their spectroscopic properties and differences in reactivity.

Experimental Section

Materials. Ferrous perchlorate hexahydrate (Alfa) was used without further purification. Diethylenetriamine (dien) was obtained from Wako. Bis(2-pyridylmethyl)amine (2-DPA) was prepared according to the method of Romary et al.,[20] using 2-(chloromethyl)-pyridine and 2-(aminomethyl)pyridine, bp 130 °C (15 mmHg). All other materials were commercially purchased and were used without further purification.

***mer*-Na[Fe(CN)$_3$(2-DPA)]·C$_3$H$_7$OH·NaClO$_4$·1.5H$_2$O (1).** To a vigorously stirred solution of Fe(ClO$_4$)$_2$·6H$_2$O (5.05 g, 14 mmol) in 15 mL of anhydrous methanol was added a solution of 2-DPA (5.55 g, 28.0 mmol in 15 mL) in methanol, under argon, at room temperature, to yield a red-brick suspension. The suspension turned to a deep orange color on the addition of an aqueous solution of NaCN (2.05 g, 42 mmol in 3.2 mL). The reaction mixture was stirred for 1 h and concentrated to near dryness under reduced pressure at a temperature below 40 °C. To the resulting red-brown solid was added 120 mL of *n*-propanol, the mixture was vigorously shaken, and the resulting suspension was cooled on an ice−water bath for 1 h. The insoluble yellow precipitate was collected on a filter and washed successively with *n*-propanol (30 mL) and ether (6 mL). The product was then dried and stored in vacuo. Yield: 5.58 g (71%).

A 500 mg portion of the crude product was suspended in *n*-propanol and ground with a mortar and the insoluble material collected on a filter. This procedure was repeated to give a sample which showed a constant visible spectrum. Yield: 302 mg (60.4%). ^{1}H NMR (D$_2$O): δ 0.896 (t, CH$_3$), 1.550 (q, CH$_3$C*H*$_2$), 3.544 (t, C*H*$_2$OH), 4.525 (d, J = 15.4 Hz, CHH), 4.595 (d, J = 15.4 Hz, CHH), 7.030 (t), 7.128 (d, J = 7.3 Hz), 7.551 (t, J = 7.3 Hz), 8.303 (d, J = 4.9 Hz). ^{13}C NMR (D$_2$O, int ref dioxane = 67.4 ppm): δ 58.08 (CH$_2$), 120.38, 124.05, 136.56, 156.17. Anal. Calcd for Na[Fe(CN)$_3$(2-DPA)]·C$_3$H$_7$OH·NaClO$_4$·1.5H$_2$O: C, 38.29; H, 4.11; N, 14.88. Found: C, 39.07; H, 4.31; N, 14.92. IR (selected band in cm^{-1}): 2057 (vs), 2053 (vs).

***fac*-Na[Fe(CN)$_3$(2-DPA)]·0.75NaClO$_4$ (2).** An ampule containing an aqueous solution of *mer*-Na[Fe(CN)$_3$(2-DPA)]·C$_3$H$_7$OH·NaClO$_4$·1.5H$_2$O (4.45 g, 7.9 mmol) in 18 mL was sealed under vacuum after three freeze−thaw cycles. The ampule was warmed for 18 h at 50 °C and then cooled to room temperature. The reaction mixture was filtered, and the filtrate was concentrated under reduced pressure. The resulting red solid was dissolved in anhydrous methanol (14 mL) followed by the addition of ether (15 mL); the yellow crystals that separated were collected, washed with ether (30 mL), dried, and stored in vacuo. The crude product was recrystallized by dissolving in anhydrous methanol (6 mL) followed by the addition of ether (15 mL). The resulting yellow crystals were collected on a filter, washed with ether (20 mL), dried under reduced pressure, and stored in vacuo. Yield: 1.08 g (31%). ^{1}H NMR (D$_2$O): δ 4.150 (d, J = 17.2 Hz), 4.688 (d, J = 17.2 Hz), 7.160 (t, J = 8.1 Hz), 7.237 (d, 8.1), 7.573 (t, J = 7.0 Hz), 9.167 (d, J = 5.1 Hz), 5.41 (N−H). ^{13}C NMR (int ref TSP): δ 63.6 (CH$_2$), 123.13 (C5), 126.38 (C3), 139.04 (C4), 155.65 (C6), 164.48 (C5). ^{13}C NMR (D$_2$O, int ref dioxane = 67.4 ppm): δ 61.6, 120.85, 123.99, 136.83, 153.41, 162.17. Anal. Calcd for Na[Fe(CN)$_3$(2-DPA)]·0.75NaClO$_4$: C, 40.31; H, 2.71; N, 18.80. Found: C, 39.92; H, 3.49; N, 18.58. IR (selected band in cm^{-1}): 2063 (vs), 2042 (vs).

***mer*-Na[Fe(CN)$_3$(2-DPA-2H)]·2H$_2$O (3).** To 2 mL of an aqueous solution of 587 mg (1 mmol) of *mer*-Na[Fe(CN)$_3$(2-DPA)]·C$_3$H$_7$OH·NaClO$_4$·1.5H$_2$O was added at room temperature 1 mL of an aqueous 1 M hydrogen peroxide. The resulting deep red solution was stirred for 5 min and concentrated under reduced pressure. The red colored residue was dissolved in 1 mL of water and applied to the top of a Sephadex G-15 column (2.6 cm i.d. × 80 cm) and the column eluted with water. The fractions which showed an absorption maximum at 530 nm were combined and concentrated under reduced pressure to yield red crystals, which were stored in vacuo. Yield: 39 mg (10%). ^{1}H NMR (D$_2$O): δ 5.93 (s, CH$_2$−N), 7.12 (t, J = 6.6 Hz, H5), 7.33 (t, J = 7.0, H5′), 7.36 (d, J = 8.0 Hz, H3), 7.68 (t, J = 7.7 Hz, H4), 7.81 (t, J = 7.5 Hz, H4′), 7.86 (d, J = 7.7 Hz, H3′), 8.40 (t, J = 5.1,H6), 8.55 (d, J = 5.9 Hz, H6′), 9.23 (s, azomethine). Anal. Calcd for Na[Fe(CN)$_3$(2DPA-2H)]·2H$_2$O: C, 46.18; H, 3.88; N, 21.54. Found: C, 46.15; H, 3.62; N, 21.34. IR (selected band in cm^{-1}): 2061 (vs).

***fac*-[Fe(CN)$_3$(2-DPA)]·0.5H$_2$O (4).** To a 1 mL portion of a mixture of acetic acid, methanol, and water (1:2:1 by volume) was suspended *fac*-Na[Fe(CN)$_3$(2-DPA)]·0.75 NaClO$_4$ (354 mg, 0.79 mmol). On the addition of 0.3 mL of an aqueous solution of H$_2$O$_2$ (1 M) to the suspension, the suspended Fe^{II} complexes dissolved transiently, after which yellow crystals were deposited. These crystals were collected on a filter, washed with ether, and stored in vacuo. Yield: 179 mg (66.2%). Anal. Calcd for [Fe(CN)$_3$(2-DPA)]: C, 52.81; H, 3.84; N, 24.63. Found: C, 52.86; H, 3.89; N, 24.18. IR (selected band in cm^{-1}): 2119 (vs).

Na[Fe(CN)$_3$(dien)]·3H$_2$O·0.5NaClO$_4$ (5). To a vigorously stirred solution of Fe(ClO$_4$)$_2$·6H$_2$O in 50 mL of methanol was added a methanolic solution of dien (10.3 g, 100 mmol) and the mixture stirred for 30 min at room temperature. An aqueous solution of NaCN (7.35 g, 150 mmol, in 16 mL) was then added dropwise to the vigorously stirred mixture, and the yellow crystals that separated were collected by filtration. The crude product was recrystallized from water−*n*-propanol, and the crystals were washed with *n*-propanol and ether successively and stored in vacuo. Yield: 12.35 g (65.8%). ^{1}H NMR (D$_2$O): δ 2.30−2.41 (m, 2H), 2.55−2.80 (m, 4H), 2.82−3.00 (m, 2H). Anal. Calcd for Na[Fe(CN)$_3$(dien)]·3H$_2$O·0.5NaClO$_4$: C, 22.40; H, 5.10; N, 22.39. Found: C, 22.31; H, 4.76; N, 22.16. IR (selected band in cm^{-1}): 2046 (vs), 2007 (vs).

***fac*-[Fe(CN)$_3$dien]·H$_2$O (6). 5** (2.00 g, 5.34 mmol) was dissolved in 60 mL of a mixture of acetic acid−methanol−water (1:2:1). The mixture was stirred in an ice bath, and 30% hydrogen peroxide was added. The separated crystals were collected on a filter. This crude product was suspended in 1 M hydrochloric acid, whereupon the small crystals changed into well-defined yellow crystals. These crystals were collected by filtration and washed with ether. Yield: 1.15 g (84.3%). Anal. Calcd for [Fe(CN)$_3$dien]·H$_2$O: C, 32.96; H, 5.93; N, 32.95. Found: C, 32.94, H, 5.86, N, 32.91. IR (selected band in cm^{-1}): 2130 (vs), 2103 (vs).

Physical Measurements. Electronic spectra of solutions of the Fe(II) and Fe(III) complexes, in hydrochloric acid (1.0×10^{-3} M), were recorded with a Shimadzu UV-2200 spectrophotometer. Infrared spectra were recorded with a JEOL JIR-6500 FT-IR spectrophotometer using KBr disks. ^{1}H and ^{13}C NMR spectra of the Fe(II) complexes were measured by dissolving a weighed sample (15−20 mg) in D$_2$O (0.35 mL) containing sodium 3-(trimethylsilyl)propionate-2,2,3,3-d_4 as an internal standard (−0.02 ppm for ^{1}H NMR and −1.91 ppm for ^{13}C NMR) degassed by several freeze−pump−thaw cycles, followed by sealing in a 5-mm-

(19) Goto, M.; Koga, N.; Ohse, Y.; Kurosaki, H.; Komatsu, T.; Kuroda, Y. *J. Chem. Soc., Chem. Commun.* **1994**, 2015−2016.
(20) Romary, J. K.; Barger, J. D.; Bunds, J. E. *Inorg. Chem.* **1968**, *7*, 1142−1145.

diameter tube. ^{1}H and ^{13}C NMR spectra were recorded on either a JEOL JNM-GX-400 or a JEOL JNM-EX270 spectrometer.

Kinetic Measurements. Experiment 1. Isomerization of *mer*-[Fe(CN)$_3$(2-DPA)]$^-$ to *fac*-[Fe(CN)$_3$(2-DPA)]$^-$. *mer*-Na[Fe(CN)$_3$-(2-DPA)]·C$_3$H$_7$OH·NaClO$_4$·1.5H$_2$O (6.7 mg, 0.01 mmol) was dissolved in 50 mL of water. This solution, under an argon atmosphere, was placed in a thermostated bath. At appropriate intervals (typically 30 min), a sample was withdrawn and its visible spectrum was recorded with a Shimadzu-UV2200 spectrophotometer. From the slope of the plots of $\ln[(\text{abs}_t - \text{abs}_\infty)/(\text{abs}_0 - \text{abs}_\infty)]$ against time, the first-order rate constant for the isomerization was obtained.

Experiment 2. An aqueous solution of *mer*- or *fac*-[Fe(CN)$_3$-(2-DPA)]$^-$ in a buffered solution (50 mM phosphate buffer) was placed in an optical cell in a spectrophotometer that was maintained at a constant temperature by a circulating thermostated water. A buffered aqueous solution of ammonium peroxodisulfate was added to the Fe(II) solution, and the change in absorbance at 530 nm for the *mer*- and that at 380 nm for the *fac*-isomer was recorded. The initial velocity was obtained by $\upsilon_0 = (1/\epsilon_{530})(\Delta\text{abs}/\Delta t)_{t=0}$ for the *mer* and $\upsilon_0 = (1/\Delta\epsilon_{380})(\Delta\text{abs}/\Delta t)$ for the *fac*-isomer, where ϵ_{530} is the molar absorption coefficient of the [Fe(CN)$_3$(*mer*-2DPA-2H)]$^-$ and $\Delta\epsilon_{380}$ the difference between the molar absorption coefficients of *fac*-[Fe^{III}(CN)$_3$(2-DPA)] and *fac*-[Fe^{II}(CN)$_3$(2-DPA)]$^-$.

Electrochemical Measurements. Cyclic voltammetry measurements were obtained with a BAS model CV-27 voltammograph and a Riken Denshi F-3EH XY recorder using a saturated Ag−AgCl electrode as a reference electrode and glassy carbon and a platinum wire as the working and auxiliary electrodes, respectively. Measurements were made on solutions containing 10^{-3} M iron complex using 0.1 M NaCl as a supporting electrolyte; argon was passed through the solution for 10 min prior to the measurements.

Crystallographic Data Collection and Refinement of the Structure of [Fe(CN)$_3$(dien)]·H$_2$O (6). The diffraction intensities of a yellow crystal of **6** with approximate dimensions of 0.44 × 0.21 × 0.06 mm were collected with graphite-monochromatized Mo Kα radiation using the $\omega/2\theta$ scan technique to $2\theta_{max} = 55.0°$ on a Rigaku AFC-7R diffractomter at 293 K. A total of 2968 reflections were measured of which 2787 were unique and 1975 were included in calculation with $I > 3.00\sigma(I)$. Lorentz and polarization factors were applied, but no correction was made for absorption. Cell parameters were obtained by the least-squares refinement of the setting angles of 25 reflections with $2\theta = 26.0-32.2°$ (λ(Mo Kα) = 0.710 69 Å).

The structure was solved by direct methods using SAPI91[21] and refined by the full-matrix least-squares method to final residuals of $R = 0.033$ and $R_w = 0.033$ with weights based on counting statistics. Hydrogen atoms were placed in the calculated positions but were not refined. All calculations were performed with the teXsan crystallographic software package,[22] and scattering factors were taken from ref 23. Crystallographic data and details of the data collection and structure refinements can be found in Table 1.

Table 1. Summary of Crystallographic Data for [Fe(CN)$_3$(dien)]·H$_2$O (**6**)

empirical formula	$FeC_7N_6H_{15}O$
fw	253.07
cryst syst	monoclinic
space group	$P2_1/n$
a, Å	8.336(4)
b, Å	13.340(5)
c, Å	10.429(3)
α, deg	90.0
β, deg	91.96(3)
γ, deg	90.0
V, Å^3	1159.1(7)
D_{calcd}, g cm^{-1}	1.450
Z	4
μ, mm^{-1}	1.286
λ, Å	0.710 69
T, K	293
no. of reflns collcd/unique	2968/2787 ($R_{int} = 0.018$)
no. of data/restraints/params	1975/0/196
refined on the basis of	F
GOF	1.37
final *R* indices[a]	$R = 0.033$ [$I > 3\sigma(I)$] $R_w = 0.033$
largest diff peak and hole, e/Å^3	0.34 and −0.26

[a] $R = \sum||F_o| - |F_c||/|F_o|$. $R_w = [\sum w(|F_o| - |F_c|)^2/\sum wF_o^2]^{1/2}$. $w = 1/\sigma^2(F_o)$.

Results

Preparation of Iron(II) and Iron(III) complexes. Mononuclear iron complexes with 2-DPA exist in two geometrical configurations: *fac* and *mer*. The successive addition of 2-DPA (2 equiv) and sodium cyanide (3 equiv) to a methanol solution of Fe(ClO$_4$)$_2$·6H$_2$O afforded a dark orange solution. After concentration of the solution to near dryness, *n*-propanol was added and the red-brown solid triturated. The undissolved yellow solid was collected by filtration and washed with *n*-propanol. This material was a mixture of *fac*- and *mer*-[Fe(CN)$_3$(2-DPA)]$^-$ complexes with the latter as the major component. After grinding of the sample with a mortar in the presence of *n*-propanol, only the *mer*-isomer (**1**) remained in insoluble form. The *fac*-isomer (**2**) was obtained by isomerization of an aqueous solution of **1** under anaerobic conditions (vide infra).

The iron(III) complex of the *fac*-isomer (**4**) was prepared by oxidation of the corresponding iron(II) complexes under acidic conditions.

The oxidation of **1** with hydrogen peroxide resulted in an intense red solution, from which the dehydrogenated product (**3**) was isolated. Similar treatment of **2** resulted in the formation of the corresponding Fe(III) complexes.

Preparation of tricyano(dien)ferrate(II) complex, **5**, was carried out on in a manner similar to that used to prepare 2-DPA by adding 3 equiv of dien to generate the bis(dien)-iron(II) complex, followed by the addition of 3 equiv of NaCN. It was necessary to carry out this procedure under an inert gas to prevent oxidation by air.

The corresponding Fe(III) complex, **6**, was prepared in a yield of 84% by oxidation with H_2O_2 under acidic conditions.

The infrared spectrum of the *fac*-isomer of iron(II) complex, **2**, showed the two intense CN stretching bands at 2042 and 2063 cm^{-1} while that of iron(III) complex **4** showed a single intense band at 2119 cm^{-1}.

Spectroscopic Properties of Iron(II) and Iron(III) Complexes. The ^{1}H NMR spectra of **1**−**3** are shown in Figure 1. Since **1** has a 2-fold axis of rotation and **2** has a mirror plane, both gave 6 signals, in addition to N−H, which

(21) SAPI91: Hai-Fu. F. *Structure Analysis Programs with Intelligent Control*; Rigaku Corp.: Tokyo, Japan, 1991.
(22) teXsan: *Crystal Structure Analysis Package*; Molecular Structure Corp.: Houston, TX, 1985 and 1999.
(23) Cromer, D. T.; Waber, J. T. *International Tables for X-ray Crystallography*; The Kynoch Press: Birmingham, England, 1974; Vol. IV, Table 2.2A.

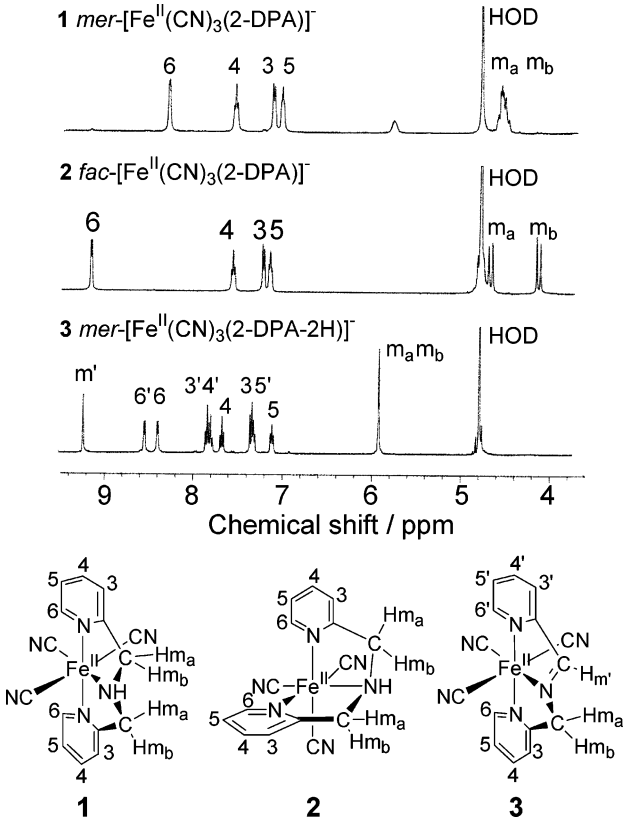

Figure 1. ^{1}H NMR spectra of tricyano(2-DPA)ferrate(II) complexes and the dehydrogenated product and their structures with the proton signals labeled.

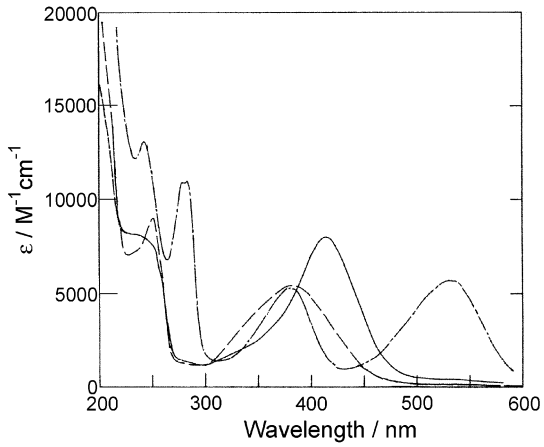

Figure 2. Electronic spectra of tricyano(2-DPA)ferrate(II) complexes in 10^{-3} M hydrochloric acid: *mer*-[Fe(CN)$_3$(2-DPA)]$^-$ (—); *fac*-[Fe(CN)$_3$(2-DPA)]$^-$ (– – –); *mer*-[Fe(CN)$_3$(2-DPA-2H)]$^-$ (– · –).

were located at 5.78 and 5.41 ppm for **1** and **2** immediately after dissolution. The assignment of geometrical isomerism was determined on the following basis: (1) larger difference in the magnetic environment of two methylene hydrogens for **2**, 4.15 and 4.68 ppm, than for **1**, 4.50 and 4.53 ppm; (2) reactivity with respect to the dehydrogenation of the Fe(III) complexes. The spectrum of **3** indicates a loss of symmetry and new singlets at 9.24 (azomethine) and 5.93 ppm (methylene).

UV−vis spectra of the iron(II) complexes in 10^{-3} M hydrochloric acid (Figure 2) showed strong absorptions at 412 nm for **1** and an asymmetric absorption at 385 nm for

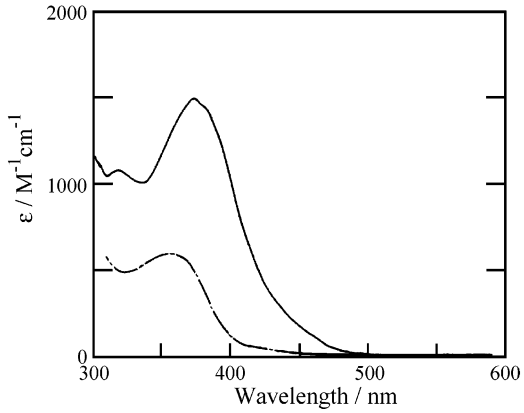

Figure 3. Electronic spectra of tricyano(triamine)ferrate(III) complexes in 10^{-3} M hydrochloric acid: *fac*-[Fe(CN)$_3$(2-DPA)] (—); *fac*-[Fe(CN)$_3$-(dien)] (– · –).

2. The bis(2-DPA)iron(II) complex has been reported to show a strong band at 432 nm (ϵ = 9000) with a shoulder at 385 nm.[24] The substitution of one molecule of 2-DPA with three cyano ligands had no effect on the position of the spectrum. These absorptions are assigned to Fe(II) to a pyridine charge-transfer band. The characteristic Fe(II) to a 1,2-diimine charge-transfer band was observed for **3** at 529 nm with a value of ϵ of 5680 as well as a band at 380 nm; an additional new strong band appeared at 283 and 279 nm with a value of ϵ of about 11 000. This band appears to be derived from the n−π transitions of pyridine which appeared at around 250 nm for **1** and **2**.

For the dien, complex **5** showed ^{1}H NMR signals in the ordinary range as well as 2-DPA (see Experimental Section), suggesting that it is also diamagnetic. UV−vis spectra of the iron(III) complexes, *fac*-isomers **4** and **6**, in 10^{-3} M hydrochloric acid (Figure 3) showed absorption maxima at λ_{max} 380 for **4** and at 360 nm for **6**, which have previously been assigned as CN^- to an Fe(III) LMCT transition.[25,26] The weak absorption at around 400 nm is assigned to an LMCT band from ligand to Fe(III), and the intensity of the absorption increases with increasing of number of pyridine rings.

X-ray Crystal Structure of [Fe(CN)$_3$(dien)]·H$_2$O (6). To confirm the structure of the [Fe(CN)$_3$(dien)] complex, the crystal structure of [Fe(CN)$_3$(dien)]·H$_2$O, **6**, was determined. The complex molecule has an octahedral geometry and belongs to a *fac*-isomer as shown in Figure 4. Table 2 summarizes selected bond distances and angles for **6**. The mean Fe−N distances (2.008 Å) are longer than the Co−N distances (1.96 Å) previously reported for *s*-*fac*-[Co(dien)$_2$]-Br$_3$[27] by 0.048 Å but smaller than that (2.073 Å) found for *s*-*fac*-[Rh(dien)$_2$]Br$_3$.[28] The bite angles of N(4)−Fe-N(5), 83.3(1)°, and N(5)−Fe-N(6), 83.5°, are narrower than the corresponding angles of the Co complexes, 86.6 and 87.2°,[27]

(24) Butcher, R. J.; Addison, A. W. *Inorg. Chim. Acta* **1989**, *158*, 211−215.
(25) Shahoua, V. E. *J. Am. Chem. Soc.* **1964**, *86*, 2109−2115.
(26) Gale, R.; McCaffery, A. J. *J. Chem. Soc., Dalton Trans.* **1973**, 1344−1351.
(27) Kobayashi, M.; Marumo, F.; Saito, Y. *Acta Crystallogr.* **1972**, *B28*, 470−474.
(28) Harada, K. *Bull. Chem. Soc. Jpn.* **1993**, *66*, 2889−2899.

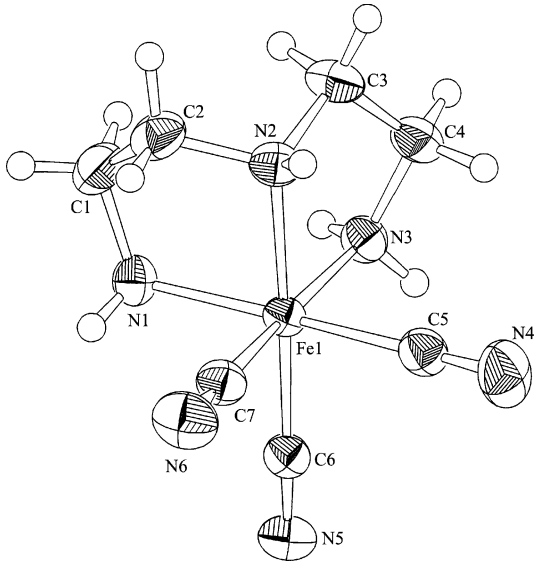

Figure 4. ORTEP diagram of *fac*-[Fe(CN)$_3$(dien)] in **6**. Thermal ellipsoids are illustrated at 30% probability.

Table 2. Selected Bond Distances (Å) and Angles (deg) for **6**

Fe−N(1)	2.009(3)	Fe−N(2)	2.018(2)
Fe−N(3)	1.998(2)	Fe−C(5)	1.930(3)
Fe−C(6)	1.931(3)	Fe−C(7)	1.938(3)
N(1)−Fe−N(2)	83.3(1)	N(1)−Fe−N(3)	95.1(1)
N(1)−Fe−C(5)	175.4(1)	N(1)−Fe−C(6)	92.2(1)
N(1)−Fe−C(7)	90.6(1)	N(2)−Fe−N(3)	83.5(1)
N(2)−Fe−C(5)	95.3(1)	N(2)−Fe−C(6)	173.9(1)
N(2)−Fe−C(7)	92.0(1)	N(3)−Fe−C(5)	89.0(1)
N(3)−Fe−C(6)	92.8(1)	N(3)−Fe−C(7)	172.2(1)
C(5)−Fe−C(6)	89.5(1)	C(5)−Fe−C(7)	85.1(1)
C(6)−Fe−C(7)	92.3(1)		

but wider that those reported for the Rh(III) complex, 81.7 and 82.4°.[28] However, the N(4)−Fe−N(6) angle (95.1°) is wider by 5.6° than that of the Co(III) complex and by 4.3° than that of the Rh(III) complex.[28] This angle is susceptible to the ligand in the complex molecule; the corresponding angle in *s-fac*-[Co(NH$_3$)(NO$_2$)$_2$]Cl is 91.38(13)°.[29] The present tricyanoiron(III) complex does not have strict restriction, but the presence of the other dien molecules make this angle narrower. Although the conformations of the two five-membered chelate rings found for the *s-fac*-isomer of the Co(III) complexes are δ and λ,[27] the conformation of the two five-membered chelate rings of the present Fe(III) complex has the same absolute conformation as has been reported for one of the two crystallographycally independent *u-fac*-[Co(dien)$_2$]$^{3+}$ [30] and *s-fac*-[Rh(dien)$_2$]$^{3+}$. The Fe−C bond distances are 1.931(3), 1.930(3), and 1.938(3) Å for Fe−C(1), Fe−C(2), and Fe−C(3), respectively, and the C≡N bond has the bond distances of 1.145−1.146 Å.

Electrochemical Properties. Cyclic voltammograms of **1**−**3** in acetate buffer (pH 4.0) are shown in Figure 5. Fe$^{2+/3+}$ quasi-reversible waves were found for **2** and **3**, while two-step processes were found for **1** with the more positive redox potential being identical with that for **3**. This indicates that

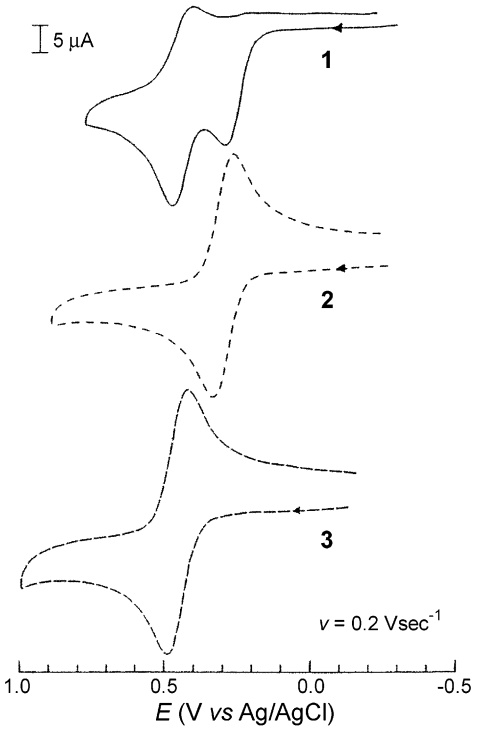

Figure 5. Cyclic voltammograms of tricyano(2-DPA)ferrate(II) complexes in acetate buffer (pH 4.0): **1**, *mer*-[Fe(CN)$_3$(2-DPA)]$^-$; **2**, *fac*-[Fe(CN)$_3$-(2-DPA)]$^-$; **3**, *mer*-[Fe(CN)$_3$(2-DPA-2H)]$^-$.

Table 3. Electrochemical Data for the Fe^{2+}/Fe^{3+} Couple of Cyano(polyamine)iron Complexes

compd	$E_{1/2}$ (NHE), V	ΔE_p, V	solvent
Fe(CN)$_6^{4-/3-}$ [a]	0.41	0.08	acetate buffer (pH 4.0), 0.1 M NaCl
Fe(CN)$_4$(en)$^{2-/-}$ [b]	0.32		
Fe(CN)$_4$(2-pyridylmethylamine)$^{2-/-}$ [b]	0.45		
fac-Fe(CN)$_3$(dien)$^{-/0}$ [c]	0.19	0.07	acetate buffer (pH 4.0), 0.1 M NaCl
mer-Fe(CN)$_3$(DPA)$^{-/0}$	0.46	0.07	acetate buffer (pH 4.0), 0.1 M NaCl
fac-Fe(CN)$_3$(DPA)$^{-/0}$	0.50	0.07	acetate buffer (pH 4.0), 0.1 M NaCl
mer-Fe(CN)$_3$(DPA-2H)$^{-/0}$	0.66	0.06	acetate buffer (pH 4.0), 0.1 M NaCl

[a] The potential was determined under the same conditions used in this study. [b] Reference 4. [c] Reference 23.

the Fe(III) complexes generated by a one electron oxidation are rapidly converted to **3** under these conditions. At pH 7 and 9, the cathode peak for **3** and the cathode peaks for **1** nearly disappeared. The electrochemical behavior is similar to those reported for tetracyanoferrate(II) complexes involving 1,2-ethylenediamine,[8] 2-aminomethylpyridine,[31] and tetraazacylotetradecatriene.[32] As expected from the kinetic measurements described below, the Fe^{III} form of **3** is unstable under basic conditions. Electrochemical data for related compounds are listed in Table 3. In the series [Fe(CN)$_{6-n}$-(N)$_n$]$^{(-4)+n/(-3)+n}$, where N denotes a simple amine donor, the redox potential decreases with *n*, but where N denotes a pyridyl nitrogen donor, the trend is reversed.

Kinetics of Isomerization of 1 to 2. Spectral changes for an aqueous solution of **1** (7.25 mg/50 mL) under degassed conditions are shown in Figure 6. A slow but clear conver-

(29) Churchill, M. R.; Harris, G. M.; Lashewysz, R. A. *Acta Crystallogr.* **1981**, *B37*, 695−697.
(30) Konno, M.; Marumo, F.; Saito, Y. *Acta Crystallogr.* **1973**, *B29*, 739−744.
(31) Toma, H. E.; Stadler, E. *Inorg. Chim. Acta* **1986**, *119*, 49−53.
(32) Toma, H. E.; da Costa Ferreira, A.; Murakami Iha, N. *Nouv. J. Chim.* **1985**, *9*, 473−478.

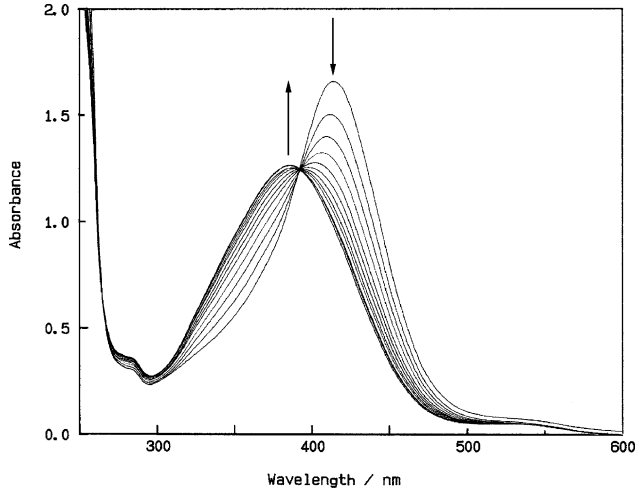

Figure 6. Spectral changes of isomerization of *mer*-$[Fe^{II}(CN)_3(2\text{-DPA})]^-$ to *fac*-$[Fe^{II}(CN)_3(2\text{-DPA})]^-$. Conditions: 0.208 mM in deaerated water at 50 °C; repetition period, 1 h.

sion of **1** to **2**, with an isosbestic point at 390 nm, can be seen. The isomerization was confirmed by changes in the ^{1}H NMR spectrum, which shows that the *fac*-isomer is favored over the *mer*-isomer in aqueous solution. The isomerization follows a first-order rate law as shown in Figure S1 (Supporting Information). The Arrhenius plots shown in Figure S2 were obtained by varying the reaction temperature, and activation parameters, $\Delta H^{\ddagger}$ of 152.9 ± 65.3 kJ mol^{-1} and $\Delta S\ddagger$ of 152.5 ± 99.9 J K^{-1} mol^{-1}, were obtained. The large activation enthalpy is compensated by the large gain in activation entropy.

Since $[Fe(phen)_3]^{2+}$ and [Fe(tetrakis(2-pyridylmethyl)-ethanediamine)]$^{2+}$ have been reported to undergo facile isomerization, it is proposed that the origin of the large enthalpy is the presence of Fe−CN bonds.[33−35]

Dehydrogenation of Coordinated 2-DPA: Coordination Mode Specificity. Spectral changes in the visible spectra of **1** and **2** in the presence of ammonium peroxodisulfate are shown in Figure 7. For **1**, the absorption at 415 nm decreased on the addition of ammonium peroxodisulfate while new absorptions appeared at 530, 380, and 280 nm with isosbestic points at 461, 383, 325, and 306 nm: thus, **1** was converted to **3** and **1** underwent oxidative dehydrogenation. On the other hand, no increase in absorption at 530 nm was found for **2** but the absorption at 395 nm decreased and the final spectrum resembled that of **4**: thus, **2** undergoes a metal-site oxidation to yield **4**, even though the reaction conditions at pH 6.51 for **1** and **2** are identical. The time course for the reaction was followed by monitoring the absorbance at 530 and 412 nm for **1** and at 380 nm for **2** while varying the pH of the medium. These results are reproduced in Figure 8. The absorption at 530 nm increased with time, reached a maximum, and then decreased, while the absorption at 412 nm showed a corresponding diminution. This time dependency shows that the dehydrogenated product, **3**, is unstable in the presence of an excess amount of the oxidizing agent, ammonium peroxodisulfate, in the neutral or basic pH region. The absorbance change for **2** showed a smooth change at 380 nm. The initial velocity was obtained from the slope at time 0 for the absorbance−time plots, and these results are listed in Table 4.

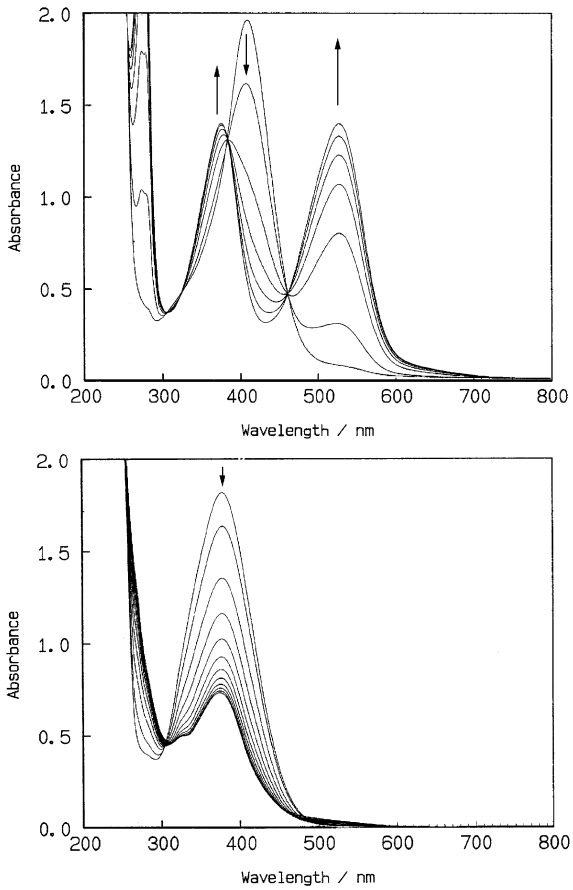

Figure 7. Spectral changes of *mer*- and *fac*-$[Fe^{II}(CN)_3(2\text{-DPA})]^-$ with $(NH_4)_2S_2O_8$ in phosphate buffer at pH 6.51: (top) *mer*-isomer, $[Fe^{II}]_0$ = 0.25 mM, $[(NH_4)_2S_2O_8]$ = 0.5 mM, repetition period = 3 min; (bottom) *fac*-isomer, $[Fe^{II}]_0$ = 0.30 mM, $[(NH_4)_2S_2O_8]$ = 0.6 mM, repetition period = 3 min.

Although the observed reactions are different in nature, i.e. dehydrogenation for **1** and metal oxidation for **2**, the initial velocity v_0 is expressed by $v_0 = k[Fe^{II}(CN)_3(DPA)^-][S_2O_8^{2-}]$ for **1** with k = 4.8 ± 0.1 M^{-1} s^{-1} and **2** with k = 2.9 ± 0.1 M^{-1} s^{-1} and no dependency on pH was found, based on the data listed in Table 4 and Figure S3.

Discussion

Tricyano(triamine)iron(II) complexes would be expected to undergo facile dehydrogenation yielding imine-coordinated Fe(II) complexes by oxidation, similar to tetracyano(diamine)ferrate(II) complexes.[4,6] In the case of tricyano(triamine)iron(II) and -iron(III) complexes, two geometrical isomers, *fac* and *mer*, would be expected. 2-DPA was used in this study because the site for dehydrogenation is restricted, due to the presence of a pyridine moiety. The

(33) Wilkins, R. G. *The study of kinetics and mechanism of reactions of transition metal complexes*; Allyn and Bacon, Inc.: Boston, MA, 1974; pp 335−360.
(34) Basolo, F.; Hayes, J. C.; Neumann, H. M. *J. Am. Chem. Soc.* **1954**, *76*, 3807−3809.
(35) Chang, H.-R.; McCusker, J. K.; Toftlund, H.; Wilson, S. R.; Trautwein, A. X.; Winkler, H.; Hendrickson, D. N. *J. Am. Chem. Soc.* **1990**, *112*, 6814−6827.

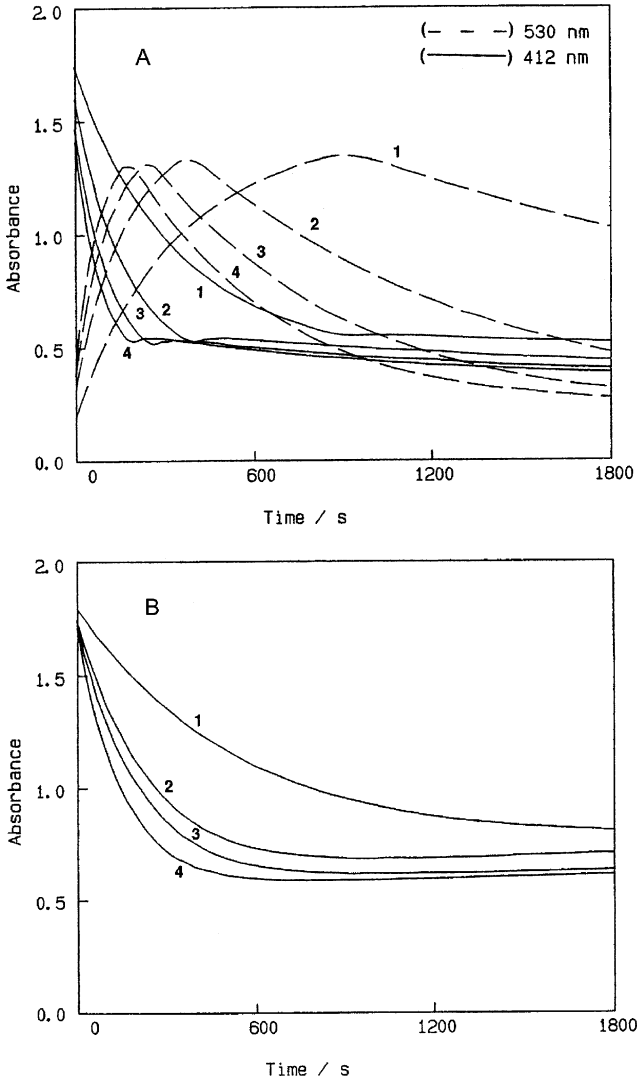

Figure 8. (A) Changes in absorbance at 530 and 412 nm with the progress of oxidative dehydrogenation of *mer*-$[Fe^{II}(CN)_3(2\text{-DPA})]^-$ in phosphate buffer at pH 7.44. $[Fe^{II}]_0 = 0.275$ mM. $[(NH_4)_2S_2O_8]$: 1, 0.5 mM; 2, 1.0 M; 3, 1.5 mM; 4, 2.0 mM. (B) Changes in absorbance at 375 nm with the progress of oxidation of central metal ion of *fac*-$[Fe^{II}(CN)_3(2\text{-DPA})]^-$ in phosphate buffer at pH 7.44. $[Fe^{II}]_0 = 0.297$ mM. $[(NH_4)_2S_2O_8]$: 1, 0.6 mM; 2, 1.2 M; 3, 1.8 mM; 4, 2.4 mM.

successive addition of DPA and sodium cyanide to a methanolic solution of $Fe(ClO_4)_2 \cdot 6H_2O$ yielded a mixture of *mer*- and *fac*-isomers. The major product was the *mer*-isomer, and advantage was taken of the difference in solubility in *n*-propanol to separate the isomers. The *mer*-isomer isomerized to the *fac*-isomer in water under anaerobic conditions with prolonged heating. This suggests that the thermodynamically stable isomer is the *fac*-isomer, at least in an aqueous solution. The corresponding tricyano(diethylenetriamine)ferrate(II) was found to exclusively yield the *fac*-isomer, and the corresponding iron(III) complex, **6**, was isolated followed by oxidation with hydrogen peroxide under acidic conditions. The crystal structure of the dien complex confirmed that it corresponds to a *fac*-isomer.

Comparison of infrared spectra between iron(II) and iron(III) complexes for *fac*-isomers, **2** and **4**, indicated that the CN stretching bands in the 2000−2100 cm^{-1} region are sensitive to the oxidation state of iron. The higher wavenumber shift by ca. 56−77 cm^{-1} in **4** reflects the shorter distance of Fe−CN in the iron(III) complex compared to iron (II) complex, **2**. In the dien complex, a similar behavior was observed: 2007 and 2046 cm^{-1} for iron(II) complex, **5**, vs 2103 and 2130 cm^{-1} for the iron(III) complex, **6**.

Table 4. Kinetic Results for the Oxidation of $[Fe(CN)_3(2\text{-DPA})]^-$

mer-isomer, 10^{-3} M	$[(NH_4)_2S_2O_8]$, 10^{-3} M	$\Delta abs/\Delta t$, 10^{-3} s^{-1}	pH	v, 10^{-6} M s^{-1}
0.279	2	14.5	6.51	2.45
	1.5	11.2		1.93
	1	8.01		1.37
	0.5	4.00		0.69
0.273	2	14.6	7.02	2.50
	1.5	10.9		1.87
	1	7.72		1.32
	0.5	3.87		0.66
0.283	2	14.7	7.98	2.52
	1.5	12.2		2.09
	1	7.86		1.35
	0.5	4.10		0.70
0.275	2	14.6	9.04	2.50
	1.5	11.5		1.98
	1	7.74		1.33
	0.5	3.94		0.68
0.275	2	15.5	10.01	2.65
	1.5	12.2		2.10
	1	8.23		1.41
	0.5	4.54		0.78
0.275	2	14.8	11.00	2.53
	1.5	11.3		1.94
	1	8.03		1.38
	0.5	4.29		0.74

fac-isomer, 10^{-3} M	$[(NH_4)_2S_2O_8]$, 10^{-3} M	$\Delta abs/\Delta t$, 10^{-3} s^{-1}	pH	v, 10^{-6} M s^{-1}
0.275	2	6.16	6.03	1.15
	1.5	4.91		0.92
	1	3.30		0.618
	0.5	1.72		0.321
0.275	2	6.04	7.05	1.13
	1.5	5.30		0.993
	1	3.26		0.611
	0.5	1.72		0.321
0.275	2	6.45	8.06	1.21
	1.5	5.07		0.950
	1	3.20		0.600
	0.5	1.87		0.350
0.275	2	6.41	9.05	1.20
	1.5	4.83		0.94
	1	3.08		0.576
	0.5	1.71		0.321

Since corresponding low-spin iron polypyridylmethylated diamines undergo rapid isomerization at room temperature on the NMR time scale, it is proposed that in the presence case the isomerization is retarded by the presence of both pyridine and cyano groups.[33] In fact the activation parameters for the isomerization are $\Delta H^{\ddagger}$ of 152.9 ± 65.3 kJ mol^{-1} and $\Delta S^{\ddagger}$ of 152.5 ± 99.9 J K^{-1} mol^{-1}. The activation enthalpy is large, and as a result, the transition state is higher in energy, although the large positive activation entropy suggests an increase in randomness. These values are consistent with the rate-determining step for the dissociation of the coordinated CN^-. The trigonal bipyramid intermediate is eventually attacked by CN^-. The trans-effect, which favors a strong coordinating ligand trans to a weak coordinating ligand, appears to operate in these systems. Thus the *mer*-isomer of

$[Fe(CN)_3(2\text{-DPA})]$ is formed as a kinetically allowed product in the preparation. An aqueous solution of **1** was unstable but isomerized completely to the *fac*-isomer **2**.

The dehydrogenation of amines coordinated to group-8 elements is well documented, but the exact mechanism for the case of iron remains unclear.[17] For the Fe(amine)system, the generation of low-spin Fe(III) complexes and the disproportionation of Fe(III) complexes to the Fe(II) complex and Fe(IV) complex or Fe(III) complex with a 1 electron oxidized ligand promoted by base are prerequisite.[4,8] We also conclude that the secondary amine site is more susceptible to dehydrogenation. In the present system, the dehydrogenation is restricted to the central secondary amine site but proceeds via the formation of a planer sp^2-hybridized nitrogen. Compounds **1** and **2** are somewhat kinetically stable, although isomerization took place but at slow rate. The kinetic results in Table 2 show that the oxidation of the central metal ion, Fe(II) to Fe(III), by peroxodisulfate ion proceeds at almost the same rate for **1** and **2** but the subsequent formation of a planar sp^2-hybridized nitrogen atom by concomitant C−H scission is only allowed for **1** and is inhibited for **2**. The reaction scheme is shown in Scheme 1. This demonstrates another principle for the dehydrogenation of amines coordinated to iron(II) or iron(III).

Scheme 1

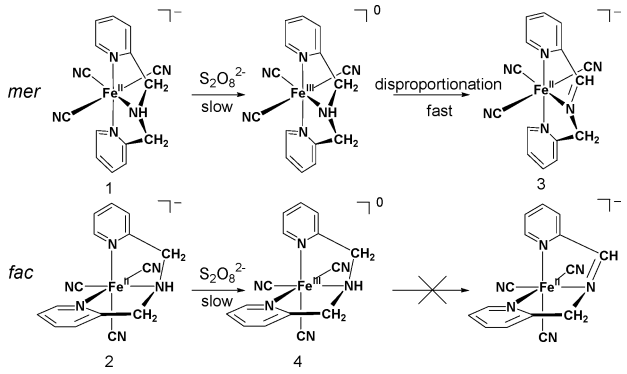

Acknowledgment. This work was supported, in part, by a Grants-in-Aid for Scientific Research Nos. 08640716 and No. 13470497 from the Ministry of Education, Culture, Sports, Science, and Technology of Japan.

Supporting Information Available: First-order rate plots for the isomerization of *mer*-$[Fe^{II}(CN)_3(2\text{-DPA})]^-$ to *fac*-$[Fe^{II}(CN)_3(2\text{-DPA})]^-$ (Figure S1), Arrhenius plots of the isomerization of *mer*-$[Fe^{II}(CN)_3(2\text{-DPA})]^-$ to *fac*-$[Fe^{II}(CN)_3(2\text{-DPA})]^-$ (Figure S2), plots of initial velocity for the oxidation of *mer*- and *fac*-$[Fe^{II}(CN)_3(2\text{-DPA})]^-$ vs $[(NH_4)_2S_2O_8]$ (Figure S3), and X-ray crystallographic details for complex **6** in CIF format. This material is available free of charge via the Internet at http://pubs.acs.org.

IC035289A